ASTONJADRO

pISSN 2302-4240
eISSN 2655-2086

Volume 15, Issue 1, March 2026, pp.059-075
DOI: http://dx.doi.org/10.32832/astonjadro.v15i1.19421 http://ejournal.uika-bogor.ac.id/index.php/ASTONJADRO

Dynamic Response of Bridge Decks to Steady State Wind Loads: A CFD Approach

Bambang Supriyadi, Andreas Triwiyono, Muhamad Farhan

Program Studi Teknik Sipil, Fakultas Teknik Sipil dan Lingkungan, Universitas Gadjah Mada Yogyakarta, INDONESIA

E-mail: bambang.supri@ugm.ac.id, muhamadfarhan@mail.ugm.ac.id

| Submitted: March 25, 2025 | Revised: October 10, 2025 | Accepted: January 10, 2026 |

| Published: March 01, 2026 |

ABSTRACT

Indonesia, as an archipelago nation located on the equator, is affected by alternating Asian and Australian monsoon systems throughout the year. The east monsoon spans from April to September, while the west monsoon occurs from October to March. In Samarinda, prevailing southern winds lead to significant fluctuations in speed and direction, impacting the stability of bridge structures. Extreme wind events pose risks to suspension bridges through aerodynamic phenomena like flutter, galloping, and vortex shedding, which impose substantial dynamic loads on the structure.This study focuses on analyzing the dynamic response of bridge decks under steady state wind loads. Daily wind data collected from January 2023 to January 2024 revealed wind speeds of 3, 4, and 5 m/s, with extreme speeds reaching 14 and 20 m/s. Steady state simulations were conducted using the simpleFoam solver in Simscale at these speeds, along with the critical velocity of 8.764 m/s derived from the bridge deck's cross-section. The simulation results provided valuable insights into pressure distributions and lateral displacement on the deck.Findings indicate that lateral displacement at a wind speed of 20 m/s reaches 1.235 m, which exceeds design limits and highlights potential structural vulnerabilities. These results demonstrate the effectiveness of steady state CFD simulations in assessing wind-induced effects on bridge structures and underline the importance of mitigation strategies to ensure stability.

Keywords: wind, bridge, vortex, resonance, displacement.

INTRODUCTION

Indonesia, as an archipelagic nation situated along the equator, experiences alternating monsoon systems throughout the year. The east monsoon occurs from April to September, while the west monsoon spans from October to March [1]. These fluctuations in wind patterns result in significant variations in speed and direction, particularly in regions like Samarinda, where prevailing winds predominantly flow from the south [2]. Such conditions present considerable risks to suspension bridges, which are highly susceptible to aerodynamic phenomena like flutter, galloping, and vortex shedding.

Vortex shedding occurs when wind flows past a bluff body, generating alternating vortices that induce oscillatory forces. The critical vortex shedding velocity is determined by the Strouhal number (St) and the dimensions of the bridge deck. When the shedding frequency aligns with the natural frequency of the structure, significant resonant oscillations may occur [3]. Historical failures like the Tacoma Narrows Bridge [4] underscore the importance of mitigating such aerodynamic instabilities.

This study investigates the effects of steady state wind loads on the aerodynamic and structural behavior of suspension bridges. Using wind speed data from BMKG (3, 4, 5, 8.764, 14, and 20 m/s), Computational Fluid Dynamics (CFD) simulations were carried out to evaluate forces and moments acting on the bridge deck. These simulation results were integrated into structural analysis using MIDAS Civil to examine displacements and frequencies, identifying potential vulnerabilities under critical wind conditions.

The novelty of this research lies in its focus on steady state CFD simulations, offering critical insights into bridge deck dynamics under consistent wind loads and their implications for structural

stability. Findings from this study contribute to advancing the understanding of vortex-induced effects and provide strategic recommendations to enhance bridge safety in regions with fluctuating wind patterns.

RESEARCH METHODS

To systematically achieve the objectives of this study, a structured research methodology was designed, integrating data collection, computational simulations, and structural analysis. This methodology ensures a comprehensive evaluation of aerodynamic effects and structural responses under steady state wind loads. The entire process is presented in a flowchart (Figure 1) that visually summarizes the sequential steps and strategies employed, allowing readers to understand the interconnection between each phase of the study.

The study begins with the collection of daily wind data, which forms the foundation for aerodynamic analyses. Wind data is sourced from BMKG and processed to determine critical speeds and variations over time. These insights feed into Computational Fluid Dynamics (CFD) simulations using the simpleFoam solver in SimScale. The CFD simulations focus on evaluating key aerodynamic parameters, including pressure distributions and structural displacements, under a range of wind speeds (3, 4, 5, 8.764, 14, and 20 m/s)

Next, the aerodynamic simulation results are integrated into structural analysis tools such as MIDAS Civil 19. This step evaluates the bridge deck's dynamic behavior, specifically identifying displacements, natural frequencies, and structural stability under steady state wind loads. Each stage of this workflow is aligned with the study's objectives, ensuring both methodological rigor and relevance.

As illustrated in Figure 1, the research workflow progresses from data collection to aerodynamic simulations, followed by structural analysis and result interpretation. This systematic approach provides the framework for achieving the study's objectives, ensuring methodological rigor and clarity.

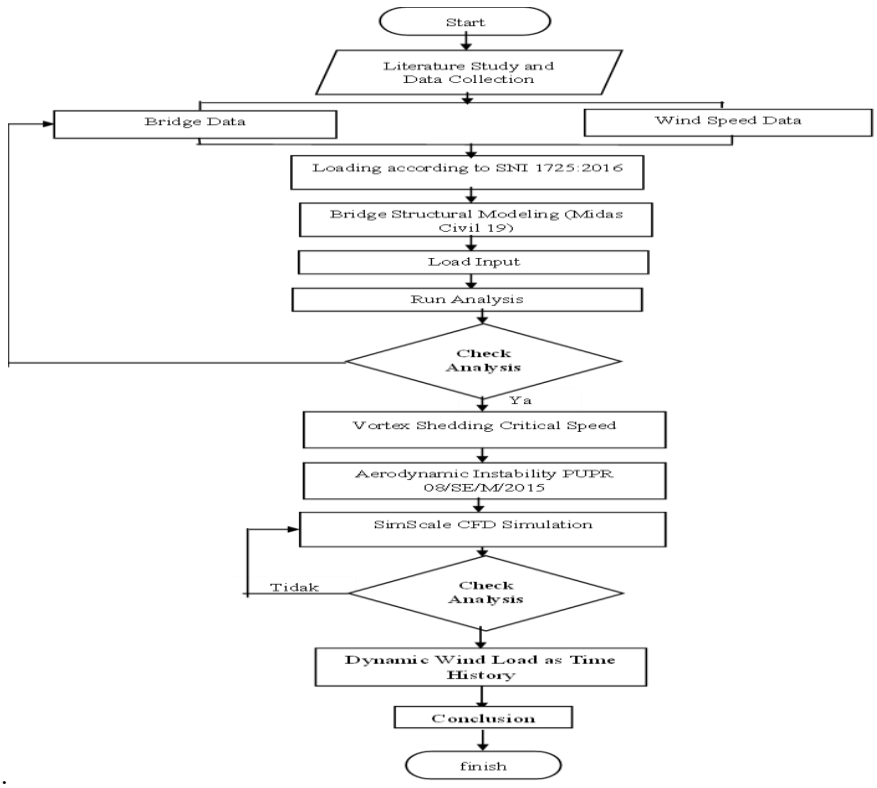

Figure 1. Flowchart of the Research Framework

pISSN 2302-4240
eISSN 2655-2086
Volume 15, Issue 1, March 2026, pp.059-075
DOI: http://dx.doi.org/10.32832/astonjadro.v15i1.19421 http://ejournal.uika-bogor.ac.id/index.php/ASTONJADRO

The results are analyzed to draw conclusions about the structural behavior of the bridge, focusing on stability and potential vulnerabilities. The workflow concludes with the interpretation of findings and recommendations for mitigation strategies to enhance bridge safety. Figure 1 depicts the overall methodology as a cohesive process, guiding the reader through the sequential steps. This systematic approach ensures the achievement of the study's objectives with clarity and precision.

Bridge Data and Specifications

The object of this research is the Kutai Kartanegara Bridge, which spans the Mahakam River, connecting Tenggarong in the west and Tenggarong Seberang towards Samarinda in the east. The study aims to analyze the dynamic response of wind flow and its impact on the structural stability of the bridge, particularly to understand the conditions contributing to its collapse in 2011.

The key technical specifications of the Kutai Kartanegara Bridge are summarized below:

- Number of Lanes : 2
- Sidewalk width : 1 meter
- Bridge width : 9 meter
- Main span lenght : 270 meter
- Side span lenght : 100 meter
- The pylon tower consists of a 15-meter concrete portal at the base and a 38-meter steel portal at the top, connected via baseplate and anchors [5]. The full view of the bridge, along with its structural components, is shown in Figure 3.

The full cross-sectional geometry of the bridge deck is presented in Figure 2, while the complete view of the bridge, including its structural components, is shown in Figure 3.

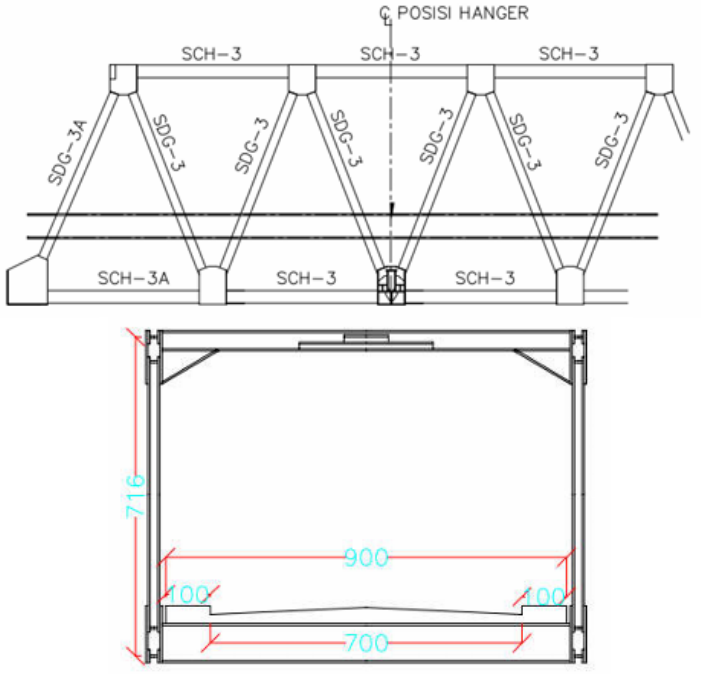

Figure 2. Cross-sectional profile of the deck [7]

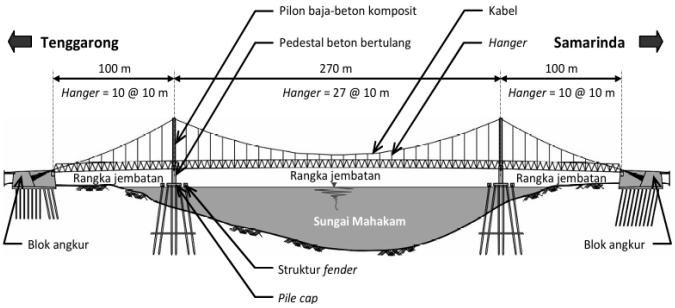

Figure 3. The full view of the Kutai Kartanegara Suspension Bridge [8]

The primary dimensions and material properties of the bridge components are detailed in Table 1. These include longitudinal beams, transverse beams, horizontal and vertical frame bars, lateral stiffeners, cables, hangers, and pylons. All structural components are fabricated using high-strength materials such as SM 490 YB, ASTM A-506, and DIN 488, with specific yield strength (Fy) and tensile strength (Fu) as outlined in the table 1

Table 1. Dimensions of the Kutai Kartanegara Bridge [6]

No	Element	Name	Profile	Quality	Fy (Mpa)	Fu (Mpa)
1	Longitudinal beam	ST-1	WF 450x200x6x12	SM 490 YB	355	490
2	Transverse beam	SGA-2	WF 800x300x12x22	SM 490 YB	355	490
3	Horizontal frame bar	SCH-3	WF 400x400x12x9	SM 490 YB	355	490
4	Vertical frame bar	SDG-3	WF 400x300x6x12	SM 490 YB	355	490
5	Lateral stifffener	UB-6A	WF 200x200x8x12	SM 490 YB	355	490
6	Wind bracing	UB-7A	WF 175x90x5x8	SM 490 YB	355	490
		UB-8A	WF 200x100x4.5x7	SM 490 YB	355	490
7	Main cable		D 258	ASTM A-506	1034.21	1516.85
8	Hanger		D 63.5	DIN 488	555	700
9	Pylon		D 609.6	ASTM A-252	241	414

Structural Modeling

The bridge was modeled in MIDAS Civil software to simulate its structural behavior under dynamic wind loads. The structural components and their respective modeling types are detailed in Table 2, while the connection types are listed in Table 3**.** The deck is represented as a stiffening truss girder, and cables are modeled with tension-only properties to reflect real-world behavior.

Table 2. Structural components and their modeling types.

Component	Structural Type	Analysis Type
Pylon Tower	Column	General structure
Pylon Beams	Beam	General structure
Main Cable	Cable	Tenssion only
Hanger Cable	Cable	Tenssion only
Deck	Stiffening Truss	Girder

Table 3. Structural connection types.

Structure 1	Structure 2	Connection 1 to 2	Connection 2 to 1
Pylon Coloumn	Pylon Beam	Full connection	Full connection
Pylon Coloumn	Main Cable	Full connection	Tenssion Only
Main Cable	Hanger Cable	Tenssion Only	Tenssion Only
Hanger Cable	Deck	Rigid link - Tenssion Only	Rigid link - Full connection

The modeling incorporates specific boundary conditions to accurately simulate the structural behavior of the Kutai Kartanegara Bridge. The pylon bases are designed as fixed supports to restrict spatial deformation and prevent rotation, ensuring structural stability at their foundations. The main cable ends are modeled as hinges, allowing limited translational movement while prohibiting rotational freedom, reflecting realistic cable behavior. For the deck supports, beam ends at the bridge

pISSN 2302-4240
eISSN 2655-2086
Volume 15, Issue 1, March 2026, pp.059-075
DOI: http://dx.doi.org/10.32832/astonjadro.v15i1.19421 http://ejournal.uika-bogor.ac.id/index.php/ASTONJADRO

supports are configured with a combination of pins and rollers. This setup provides longitudinal movement on the Samarinda side while enabling rotational freedom on the Tenggarong side [8].

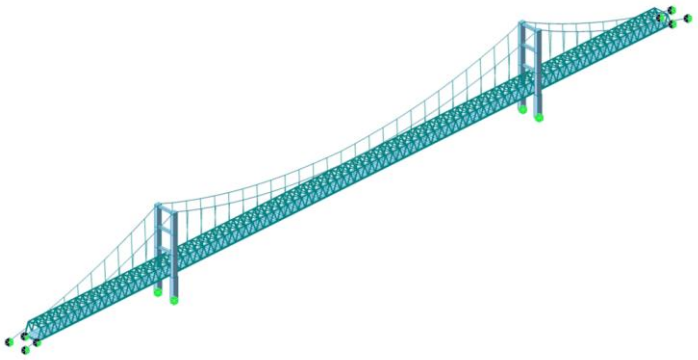

Figure 3 Bridge Modeling with MIDAS CIVIL

Wind Speed Data

The wind speed data used in this research was sourced from the Indonesian Meteorology, Climatology, and Geophysics Agency (BMKG) [2]. Analysis of the data revealed that the most frequent wind speeds fall within the range of 3 m/s, 4 m/s, and 5 m/s under typical conditions, as shown in Figure 4 and Figure 5. Extreme wind speeds recorded during the observation period reached 14 m/s and 20 m/s, predominantly originating from the south.

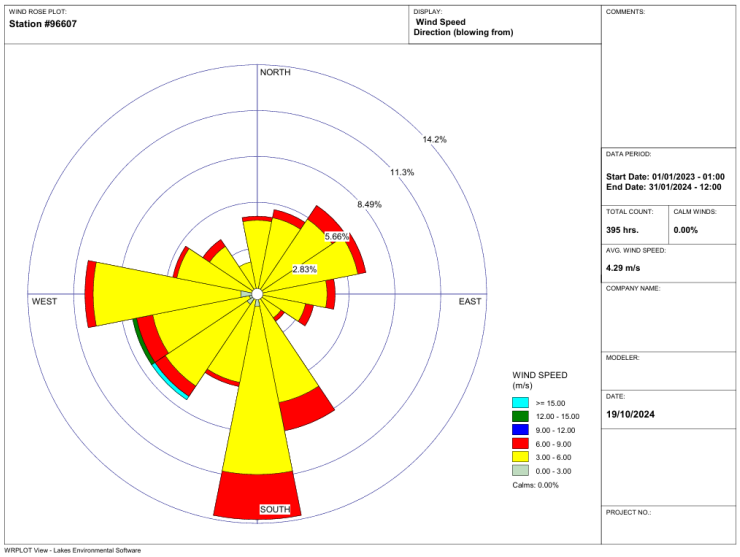

Figure 4 Wind Speed Plot with WRPlot

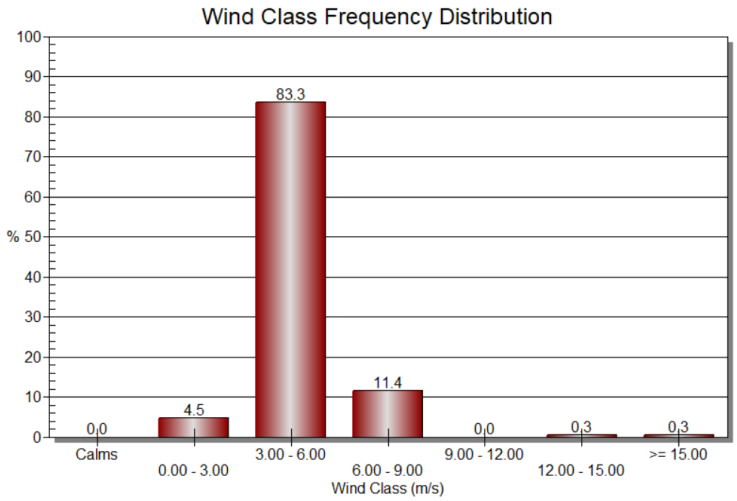

Figure 5 Wind Frequency with WRPlot

The wind directions affecting the Kutai Kartanegara Bridge are shown in Figure 6, highlighting the dominant influence of southern winds on the structural stability of the bridge [8]. The critical vortex shedding velocity, calculated based on the cross-sectional dimensions of the bridge deck, is 8.764 m/s. This value represents the critical wind speed at which vortex-induced oscillations align with the natural frequency of the bridge structure, posing significant risks of resonance.

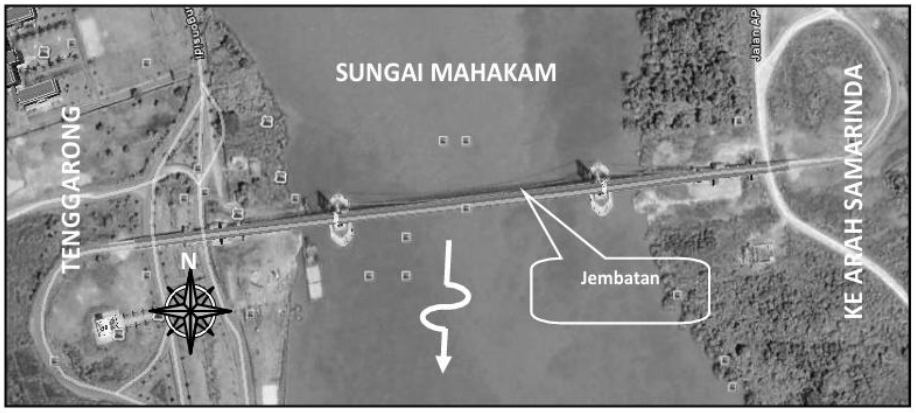

Figure 6 Wind Direction of Kutai Karta Negara Bridge [8]

These wind speeds were incorporated into the Computational Fluid Dynamics (CFD) simulations to evaluate aerodynamic forces (lift, drag, and moment) and their effects on the bridge structure.

Structural Loadings

The bridge loading follows the Indonesian National Standard [9], which considers various load types applied to the bridge structure. The loading scheme used in this study includes the following:

1. Dead Load (MS)
2. Additional Dead Load (MA)
3. Live Load (BGT, BTR, TT)
4. Wind Load (wind loads on the structure, vertical wind forces, and wind forces on vehicles

The wind load at the basic wind speed was converted into design wind speed at the elevation level (V_{dz}) using Equation 1:

$$\boldsymbol{V_{Dz} = 2.5V_0\left(\frac{V_{10}}{V_B}\right)\ln\left(\frac{Z}{Z_0}\right)} \quad 1$$

The design wind pressure (P_D) is then derived using Equation 2 :

$$\boldsymbol{P_D = P_B \left(\frac{V_{DZ}}{V_B}\right)^2} \quad 2$$

Where:
V_{DZ}: Design wind speed at elevation Z (km/h).
V_{10}: Wind speed measured at 10,000 mm above the ground or water surface (km/h)
V_B: Wind speed at 1,000 mm elevation, typically ranging from 90 to 126 (km/h)
Z: Structure elevation from the ground or water surface
V_0: Friction wind speed based on meteorological characteristics
Z_0: Upstream friction length for the bridge
P_B: Base wind pressure (MPa).
The wind load pressure values (P_D) were adjusted to a minimum of 4.4 kN/m for compression and 2.2 kN/m for tension when below the threshold values. The resulting design wind speed and pressure values are summarized in Table 4**.**

Table 4. Wind Load Pressure for Design Speeds

V_{dz1} (km/h)	V_{dz2} (km/h)	q_{EWsh} (kN/m) 90 km/h		q_{EWsh} (kN/m) 126 km/h	
		compression	tension	compression	tension
22.800	16.286	4.400	2.200	4.400	2.200
30.400	21.714	4.400	2.200	4.400	2.200
38.000	27.143	4.400	2.200	4.400	2.200
106.400	76.000	10.808	3.603	4.400	2.200
151.999	108.571	22.056	7.352	5.741	1.914

Subsequently, line loads were converted into point loads to facilitate numerical modeling and simulation in MIDAS Civil software. This step ensures proper representation of the distributed loads in the structural analysis, allowing the evaluation of displacements and stability under combined load conditions.

CFD Modeling

Computational Fluid Dynamics (CFD) is a cost-effective and flexible tool for analyzing wind-structure interactions compared to traditional wind tunnel testing. Studies by [10] and [11] validate the reliability of CFD simulations for evaluating aerodynamic forces and moments under various wind scenarios. In this study, CFD simulations were conducted using steady-state conditions to analyze the aerodynamic effects on the Kutai Kartanegara Bridge.

The Computational Fluid Dynamics (CFD) simulations were conducted using steady-state conditions to analyze the aerodynamic effects on the Kutai Kartanegara Bridge. The simulations employed the turbulence model $k-\omega$SST, with a structured external flow volume box of 50 meters in length, as recommended [12]. Boundary conditions were carefully defined to ensure accurate results: a velocity inlet was applied at the entry boundary to specify the wind speed, while a pressure outlet was set at the exit boundary to maintain atmospheric pressure. The walls of the external flow box were treated as slip walls, except for the girder's surface, where a no-slip condition was applied to capture the interaction between airflow and the deck. The wind speeds used in the simulations ranged from 3 m/s to 20 m/s, including the critical vortex shedding velocity of 8.764 m/s, calculated following the BS [13] and BSI [14] standards.

The simulations produced aerodynamic forces and moments in three axes: force (X), force (Y), and force (Z), along with moment (X), moment (Y), and moment (Z). These forces and moments were extracted at the bridge deck to serve as input data for subsequent structural analysis. The simulations were conducted with an end time of 1,000 seconds and a time step (Δt) of 1 second, ensuring the stability of the solver and the accuracy of the steady-state analysis. The external flow setup is shown in Figure 7.

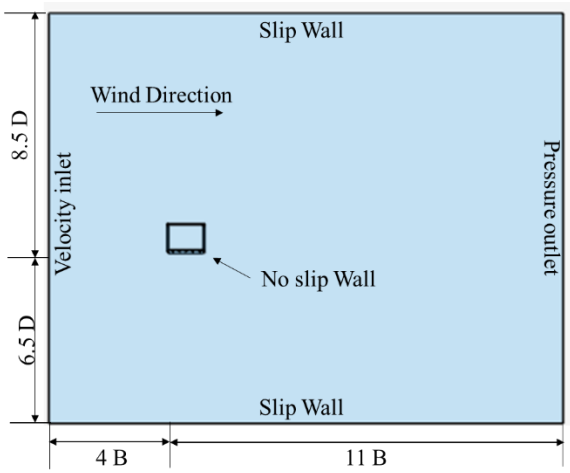

Figure 7. Modeling external flow volume boxes in SimScale

RESULT AND DISCUSSION

Natural Frequency Analysis

The initial modal analysis was conducted to identify the main vibration modes of the bridge and to ensure that the natural frequencies are outside the range that could lead to dangerous resonance when subjected to dynamic loads such as wind or traffic. The results of the modal analysis serve as the foundation for further aerodynamic evaluations and confirm the structural safety of the bridge. The natural frequencies are summarized in Table 5 below.

Table 5. The natural frequency of the bridge.

Mode Shape	Period (sec)	Frequncy (Hz)	Description
1	6.324	0.158	Symetrical Transverse Bending
2	5.308	0.188	Symetrical Vertical Bending
3	4.553	0.220	Asymetrical Torsion
4	2.947	0.339	Asymetrical Torsion
5	2.892	0.346	Symetrical Vertical Bending
6	2.248	0.445	Asymetrical Torsion
7	2.113	0.473	Symetrical Vertical Bending
8	1.813	0.552	Asymetrical Transverse Bending
9	1.792	0.558	Asymetrical Transverse Bending

For a main span of 270 meters and a total span of 470 meters, the ratio of torsional frequency to the first vertical bending frequency was calculated as 1.166, obtained from the torsional frequency of 0.220 Hz and the first vertical bending frequency of 0.188 Hz. This value does not satisfy the requirements of the Indonesian Bridge and Roadway Standards [15], which specify that the frequency ratio must be ≥ 2.5. Hence, further aerodynamic analysis is deemed necessary.

The modal analysis also revealed that the first natural period of the bridge is 6.348 seconds, which is close to the first natural period found [6], reported as 6.671 seconds. The differences were minimal, with 2.7% for mode 1, 0.7% for mode 2, and 7.5% for mode 3, demonstrate the consistency of the results obtained through the analytical methods employed in this research with those from previous studies.

Critical Vortex Shedding Velocity

The critical wind velocity v_{crit} is determined based on the first bending natural frequency (n_1), the reference width of the cross-section (b), and the Strouhal number (St). These parameters are essential in calculating the velocity at which the vortex shedding frequency aligns with the natural frequency of the structure. The equation 3 used to calculate the critical velocity is:

pISSN 2302-4240
eISSN 2655-2086
Volume 15, Issue 1, March 2026, pp.059-075
DOI: http://dx.doi.org/10.32832/astonjadro.v15i1.19421 http://ejournal.uika-bogor.ac.id/index.php/ASTONJADRO

$$v_{crit} = \frac{b.n_{i,y}}{St} \quad 3$$

The critical vortex shedding velocity was calculated as 8.764 m/s, representing the condition where the natural frequency of the structure coincides with the vortex shedding frequency. This alignment can lead to resonance and amplify the vibrational response of the structure. However, as the bridge girder employs a stiffening truss configuration, torsional critical velocity calculations are not required. Therefore, the primary focus is on the critical vortex shedding velocity for the girder.

CFD Simulation Results

The simulations were conducted under both steady state and transient conditions across a range of wind speeds: 3 m/s, 4 m/s, 5 m/s, 8.764 m/s (critical vortex shedding velocity), 14 m/s, and 20 m/s. The results encompass forces and moments acting on the bridge structure, along with visualizations of wind flow patterns (vortex shedding) occurring around the bridge deck. These patterns are illustrated in Figure 8, which depicts the aerodynamic behavior at critical velocities.

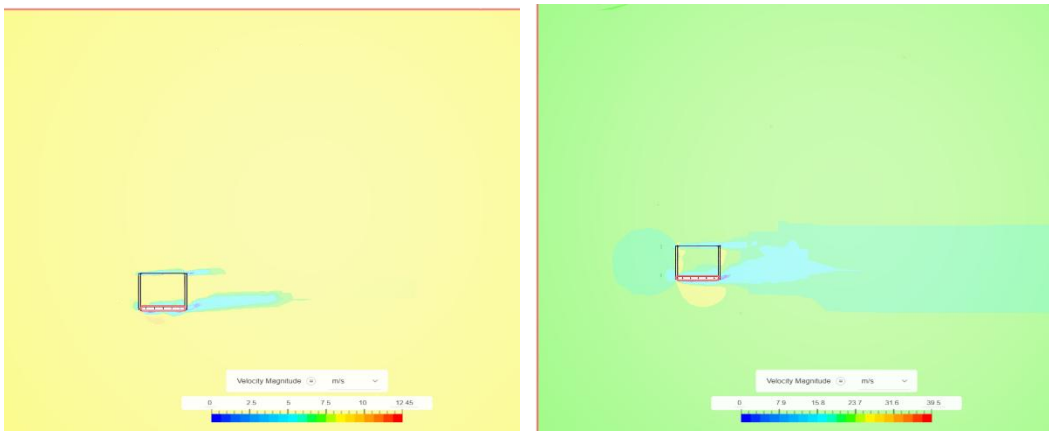

a. Vortex shedding patterns formed during the simulation at 8.764 m/s at t = 100 s

b. Vortex shedding patterns formed during the simulation at 20 m/s at t = 100 s

Figure 8 illustrates the vortex shedding patterns observed in the simulations at 8.764 m/s and 20 m/s

At wind speeds of 8.764 m/s and 20 m/s, simulated at t = 100 seconds, the vortex shedding patterns exhibit significant differences. At 8.764 m/s, the airflow forms regular and consistent vortex patterns, indicating a critical condition where resonance may occur as the vortex shedding frequency aligns with the natural frequency of the structure. Conversely, at 20 m/s, the flow becomes increasingly chaotic, reflecting extreme wind load conditions that produce larger aerodynamic forces and displacements.

These findings underscore the importance of evaluating vortex shedding at critical wind speeds and understanding the structural response under extreme wind scenarios to ensure the stability of the bridge. The forces and moments derived from these simulations are presented in Figure 9 and Figure 10, serving as essential inputs for further evaluation of the bridge's structural response:

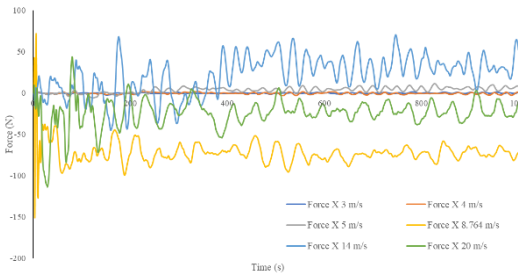

a. Steady-State Simulation – Force X

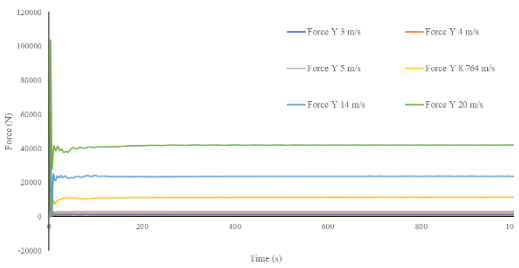

b. Steady-State Simulation – Force Y

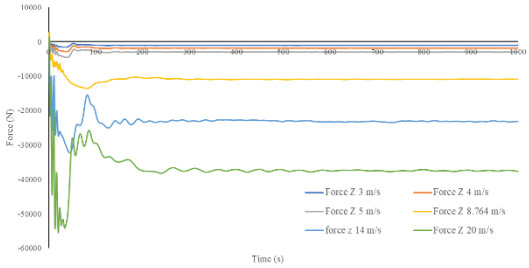

c. Steady-State Simulation – Force Z

Figure 9 Steady-State Simulation Force result

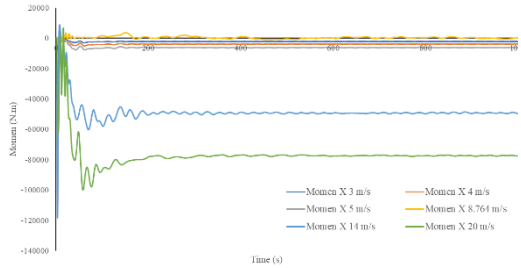

a. Steady-State Simulation – Moment X

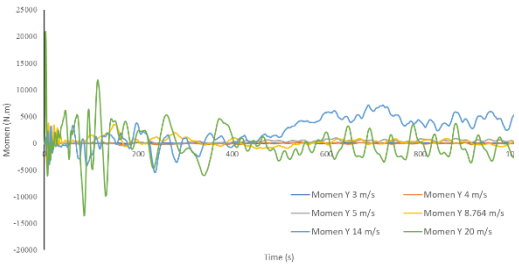

b. Steady-State Simulation – Moment Y

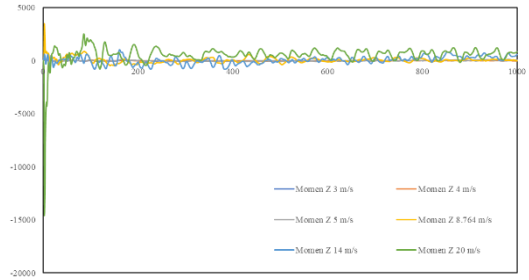

c. Steady-State Simulation – Moment Z

Figure 10 Steady-State Simulation Moment result

Structural Response
Amplitude

This subsection discusses the displacement amplitude results obtained from steady-state CFD simulations. These results were subsequently imported into MIDAS Civil for further structural analysis. The graphical outputs of displacement amplitudes along the X, Y, and Z axes are visualized in Figures 10.

pISSN 2302-4240
eISSN 2655-2086
Volume 15, Issue 1, March 2026, pp.059-075
DOI: http://dx.doi.org/10.32832/astonjadro.v15i1.19421 http://ejournal.uika-bogor.ac.id/index.php/ASTONJADRO

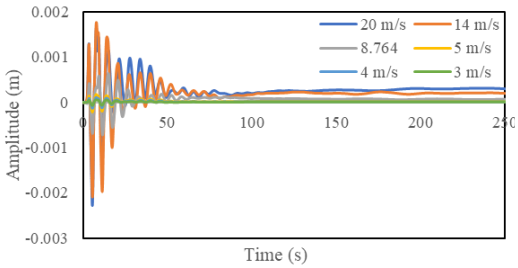

a. Displacement X Steady State

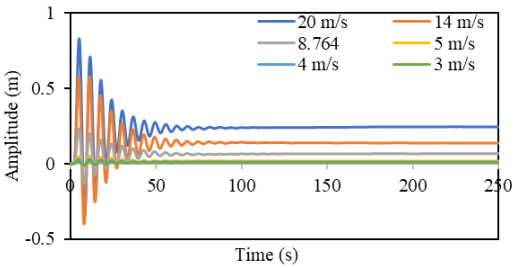

b. Displacement Y Steady State

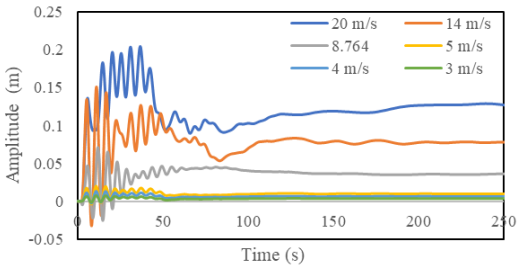

c. Displacement Z Steady State

Figure 11. Steady-state displacement results (X, Y, Z).

Frequency

The frequency responses of the structure under dynamic loading were analyzed, and the results are summarized in Figures 11 and Table 6.

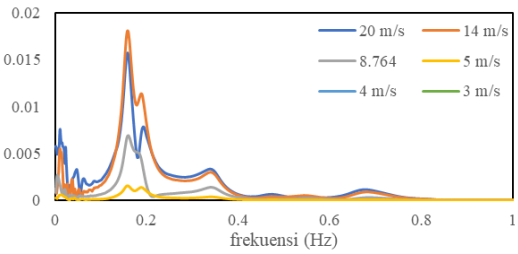

a. Frequency X Steady State

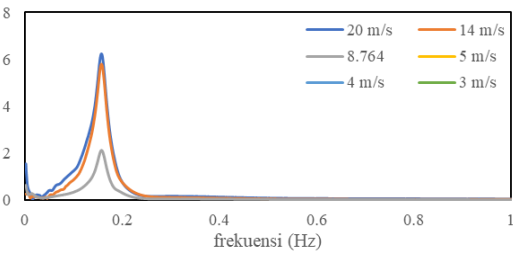

b. Frequency Y Steady State

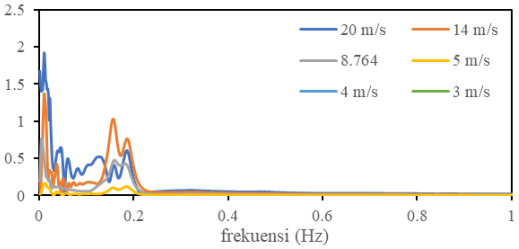

c. Frequency Z Steady State

Figure 12. Frequency responses along the X, Y, and Z axes

Table 6. Compares the amplitude and frequency responses under steady-state

Speed		Amplitude Steady State		Frequency Steady State	
		Max (m)	Min (m)	frek (Hz)	Value
3 m/s	Dx	0.0001	-0.0001	0.1587	0.0005
	Dy	0.0163	-0.0071	0.1572	0.1498
	Dz	0.0075	-0.0014	0.0137	0.0537
4 m/s	Dx	0.0001	-0.0001	0.1587	0.0009
	Dy	0.0312	-0.0151	0.1572	0.2904
	Dz	0.0130	-0.0025	0.0122	0.1043
5 m/s	Dx	0.0002	-0.0002	0.1587	0.0016
	Dy	0.0521	-0.0271	0.1572	0.4879
	Dz	0.0199	-0.0038	0.0122	0.1657
8.764 m/s	Dx	0.0006	-0.0007	0.1602	0.0069
	Dy	0.2334	-0.1309	0.1572	2.1206
	Dz	0.0711	-0.0254	0.0046	0.7648
14 m/s	Dx	0.0018	-0.0021	0.1587	0.0181
	Dy	0.5801	-0.3998	0.1572	5.8001
	Dz	0.1511	-0.0325	0.0107	1.3685
20 m/s	Dx	0.0016	-0.0023	0.1587	0.0157
	Dy	0.8301	-0.3469	0.1572	6.2411
	Dz	0.2045	-0.0015	0.0107	1.9217

Table 6 provides a detailed comparison of amplitude and frequency responses at various wind speeds under steady-state conditions. The analysis highlights key dynamic phenomena affecting the structure, with the following observations:

- The initial bending frequency of the structure is 0.188 Hz, while the initial lateral frequency is 0.158 Hz. These values serve as critical references for identifying dynamic effects on the bridge.
- The frequencies for Dx and Dy remain relatively consistent at approximately 0.1587 Hz and 0.1572 Hz, respectively, across all wind speeds, indicating stability in the natural frequency characteristics.
- In contrast, the frequency for Dz under steady-state conditions decreases from 0.0137 Hz at lower wind speeds to 0.0107 Hz at higher speeds. This variation signifies dynamic effects, such as vortex shedding, at critical wind velocities.

The amplitudes under steady-state conditions reveal significant vibrational responses due to constant wind loads:

- The maximum Dz amplitude reaches 0.2045 m at a wind speed of 20 m/s, reflecting a substantial vibrational impact on the structure.
- The variation in maximum and minimum amplitudes for Dy also demonstrates notable lateral vibrations caused by steady-state wind loads, particularly at critical speeds.

pISSN 2302-4240
eISSN 2655-2086
Volume 15, Issue 1, March 2026, pp.059-075
DOI: http://dx.doi.org/10.32832/astonjadro.v15i1.19421 http://ejournal.uika-bogor.ac.id/index.php/ASTONJADRO

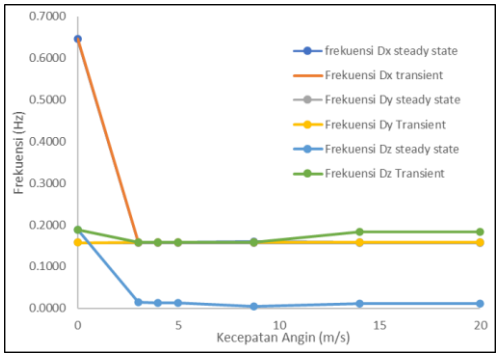

a. Frequency with wind speed graph

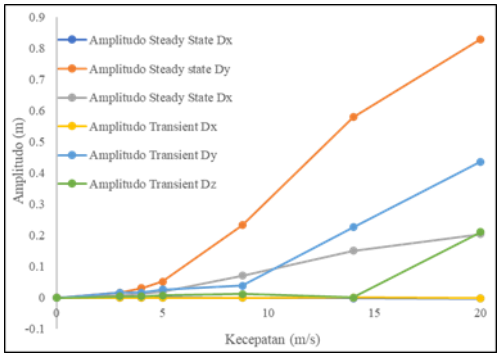

b. Amplitude with wind speed graph

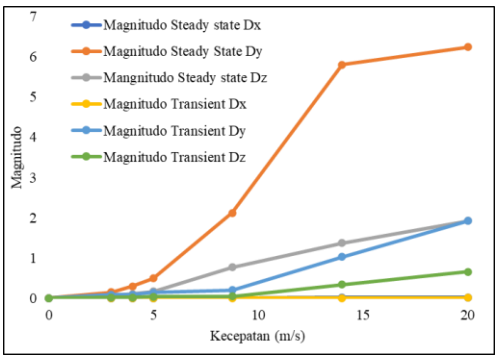

c. Magnitude with wind speed graph

Figure 13. Graph of the relationship between wind speed with (a) frequency, (b) amplitude and (c) magnitude in steady state conditions.

Figure 13 illustrates the impact of steady-state wind loads on the structure's dynamic behavior, highlighting consistent lateral frequencies and varying vertical responses. These graphical analyses complement the numerical data presented in Table 6, offering deeper insights into the dynamic characteristics and structural stability under varying wind conditions.

Vortex Shedding Effects

The maximum amplitude caused by vortex shedding was manually calculated using the formulas specified in BSI**.** For vertical bending vibrations, the equation 4 is as follows:

$$y_{max} = \frac{c b^{0.5} {d_4}^{2.5} . \rho}{4 m \delta_s} \quad (4)$$

where c is derived from Equation 5:

$$c = \frac{3(k + h\phi_s)}{d_4} \quad (5)$$

The maximum amplitude of vortex shedding depends on parameters like fascia beam thickness (k), parapet height (h), solidity ratio (ϕ_s), bridge deck width (b), and others. The calculated maximum amplitude at the critical vortex shedding velocity is 0.2475 m, while the steady-state maximum amplitude is 0.2334 m, with a percentage difference of 2.93%, validating the simulation results.

Comfort Criteria

Vortex shedding, as a dynamic phenomenon, significantly impacts the stability and safety of bridge structures. Using the comfort criteria outlined in BSI**,** the maximum amplitude and bending frequency (n_{bi}) were used to calculate a comfort level index (K_D) using Equation (6):

$$K_D = y_{max} {n_{bi}}^2 \quad 6$$

The calculated comfort levels for varying wind speeds are presented in Table 7, showing the transition from "Tolerable" conditions at lower wind speeds (3–5 m/s) to "Unpleasant" conditions at higher wind speeds (8.764,14 and 20 m/s). This highlights the critical importance of addressing vortex shedding in structural design.

Table 7. vortex shedding effect criteria

	3 m/s	**4 m/s**	**5 m/s**	**8.764 m/s**	**14 m/s**	**20 m/s**
ymax (mm)	16.303	31.234	52.137	233.445	580.137	830.132
KD (mm/s2)	0.578	1.107	1.849	8.277	20.570	29.434
	Tolerable	Tolerable	Tolerable	Unpleasent	Unpleasent	Unpleasent

Structural Displacement

This subsection discusses the structural displacement of the bridge under steady-state conditions, focusing on the effects of wind loads as per Badan Standardisasi Nasional. The analysis aims to understand the structural response under wind loads in various conditions and to ensure that displacement remains within safety limits set by the standards.Table 8 summarizes the bridge displacement results under steady-state wind load simulations for different wind speeds, and Figure 12 illustrate the displacement along the X, Y, and Z axes.

Table 8. Bridge displacement under wind load simulation

Wind Speed (m/s)		**DX (m)**	**DY (m)**	**DZ (m)**	**RX (rad)**	**RY (rad)**	**RZ (rad)**
3 m/s	VB (90 km/hours)	-0.0001	0.1979	0.0126	-0.0051	0.0000	0.0000
	VB (126 km/ hours)	-0.0001	0.1979	0.0126	-0.0051	0.0000	0.0000
	Steady State	-0.0001	0.0163	0.0075	-0.0001	0.0000	0.0000
4 m/s	VB (90 km/ hours)	-0.0001	0.1979	0.0126	-0.0051	0.0000	0.0000
	VB (126 km/ hours)	-0.0001	0.1979	0.0126	-0.0051	0.0000	0.0000
	Steady State	-0.0001	0.0312	0.0130	-0.0003	0.0000	0.0000
5 m/s	VB (90 km/ hours)	-0.0001	0.1979	0.0126	-0.0051	0.0000	0.0000
	VB (126 km/ hours)	-0.0001	0.1979	0.0126	-0.0051	0.0000	0.0000
	Steady State	-0.0002	0.0521	0.0199	-0.0005	0.0000	0.0000
8.764 m/s	VB (90 km/ hours)	-0.0001	0.1979	0.0126	-0.0051	0.0000	0.0000
	VB (126 km/ hours)	-0.0001	0.1979	0.0126	-0.0051	0.0000	0.0000
	Steady State	-0.0007	0.2334	0.0711	-0.0033	0.0000	0.0000
14 m/s	VB (90 km/ hours)	-0.0003	0.4302	0.0273	-0.0112	0.0000	0.0000
	VB (126 km/ hours)	-0.0001	0.1979	0.0126	-0.0051	0.0000	0.0000
	Steady State	-0.0021	0.5801	0.1511	-0.0062	0.0000	-0.0001
20 m/s	VB (90 km/ hours)	-0.0006	0.8763	0.0546	-0.0228	0.0000	0.0000
	VB (126 km/ hours)	-0.0002	0.2293	0.0146	-0.0059	0.0000	0.0000
	Steady State	-0.0023	0.8301	0.2045	-0.0042	0.0000	-0.0001

pISSN 2302-4240
eISSN 2655-2086
Volume 15, Issue 1, March 2026, pp.059-075
DOI: http://dx.doi.org/10.32832/astonjadro.v15i1.19421 http://ejournal.uika-bogor.ac.id/index.php/ASTONJADRO

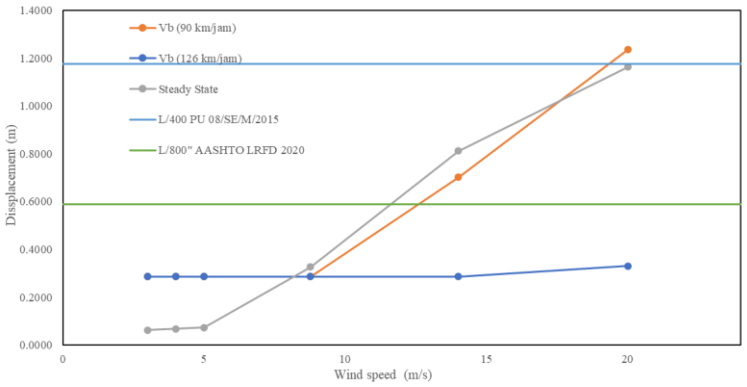

Figure 14. Displacement graph of Y axes of various wind load simulations.

Under steady-state conditions, the structural displacement of the bridge is most pronounced in the lateral direction (DY) compared to the vertical (DZ) or longitudinal (DX) directions, indicating that constant wind loads have a significant impact on lateral stability. At a wind speed of 20 m/s, the maximum lateral displacement reached 0.8301 m, a value that approaches the allowable deflection limit of L/400L/400 (1.175 m) as specified [16], but exceeds the stricter limit of L/800L/800 (0.588 m) set by the AASHTO LRFD Bridge Design Specification [17]. These findings raise concerns about the safety and stability of the bridge under such conditions. Additionally, the lateral displacement (DY) increases with wind speed, emphasizing the need for careful structural evaluations under varying wind loads.

The simulations further reveal that wind speeds with a basic velocity of 90 km/h produced higher lateral displacement compared to those at 126 km/h. This suggests that assumptions about wind load standards, as per Badan Standardisasi Nasional [9], play a critical role in influencing structural behavior. These results align with prior research by Sitanggang, which also identified structural vulnerabilities under similar conditions. The consistent increase in lateral displacement with wind speeds highlights the importance of addressing lateral forces during bridge design to ensure stability and compliance with safety standards.

CONCLUSION

This study investigated the structural displacement and dynamic response of a cable-stayed bridge under steady-state wind load conditions in accordance with Badan Standardisasi Nasional. The results revealed that the torsional-to-vertical bending frequency ratio was 1.166, falling short of the minimum standard of 2.5 outlined in Pedoman Bidang Jalan dan Jembatan, indicating a potential structural vulnerability. The critical vortex shedding velocity of 8.764 m/s was identified as a significant factor, with wind speeds of 4 m/s, 5 m/s, and 8.764 m/s requiring special attention, and 20 m/s posing a critical threat as classified under Surat Edaran Menteri Pekerjaan Umum dan Perumahan Rakyat. Displacement analysis showed that lateral displacement (DY) was the most critical, reaching a maximum of 0.8301 m at 20 m/s under steady-state conditions. While this value was within the allowable deflection limit of L/400L/400 (1.175 m), it exceeded the stricter L/800L/800 (0.588 m) limit set by AASHTO LRFD Bridge Design Specification (2020), highlighting safety concerns. Furthermore, wind loads based on SNI specifications demonstrated that a basic wind velocity of 90 km/h produced greater lateral displacement compared to 126 km/h, emphasizing the role of standard load assumptions in structural behavior. The maximum amplitude at the critical vortex shedding velocity was 0.2475 m, a mere 2.93% difference from the steady-state value of 0.2334 m, validating the reliability of simulation results. Initial vibrational frequencies of 0.188 Hz (bending) and 0.158 Hz (lateral) were observed, and lateral displacement consistently increased with higher wind speeds, underlining the importance of addressing vortex shedding effects and lateral forces in bridge design to ensure compliance with safety standards and structural stability.

ACKNOWLEDGEMENT

The authors would like to express their sincere gratitude to Universitas Gadjah Mada, particularly Fakultas Teknik, Departemen Teknik Sipil, for their support and resources that made this research possible. This study greatly benefited from the guidance and facilities provided during its implementation.

REFERENCES

[1] Y. D. Haryanto. (2024). "Effect of Monsoon Phenomenon on Sea Surface Temperatures in Indonesian Throughflow Region and Southeast Indian Ocean," *J. Southwest Jiaotong Univ.*, vol. 56, no. 6, pp. 914–923, 2021, doi: 10.35741/issn.0258-2724.56.6.80.

[2] BMKG. (2024)."Kecepatan Angin Harian," 2024. https://dataonline.bmkg.go.id/dataonline-home (accessed Aug. 22, 2024).

[3] A. Desai, S. Mittal, and S. Mittal. (2020). "Experimental investigation of vortex shedding past a circular cylinder in the high subcritical regime," *Phys. Fluids*, vol. 32, no. 1, 2020, doi: 10.1063/1.5124168.

[4] A. S. Carriols. (2015). "Vortex-induced vibrations on bridges The interaction mechanism in complex sections and a new proposed semi-empirical model," no. November, pp. 1–192, 2015.

[5] U. G. M. Tim Investigasi Runtuhnya Jembatan Kutai Kartanegara. (2011). "Investigasi Runtuhnya Jembatan Mahakam II Tenggatong Kabupaten Kutai Kartanegara Propinsi Kalimantan Timur," 2011. [Online]. Available: https://smallbusiness.chron.com/improve-customer-service-restaurant-40461.html

[6] A. N. Sitanggang and B. Piscesa. (2012). "Analisa Struktur Atas Jembatan Kutai Kartanegara Sebelum Mengalami Keruntuhan," pp. 1–5, 2012.

[7] I. E. S. Hadjoh (2016). "Analisis Kestabilan Jembatan Gantung Dengan Variasi Rasio Bentang Terhadap Lebar Jembatan," UNIVERSITAS GADJAH MADA, 2016.

[8] S. P. Mangkoesoebroto. (2012)."Keruntuhan Jembatan Gantung Kartanegara Tragedi dalam Proses Rancang Bangun Infrastruktur Sindur," vol. 19, no. 3, p. 207, 2012.

[9] Badan Standardisasi Nasional. (2016). *Pembebanan untuk jembatan*. 2016.

[10] M. Zhang, T. Wu, and F. Xu. (2018). "Vortex-induced vibration of bridge decks: Describing function-based model," *J. Wind Eng. Ind. Aerodyn.*, vol. 195, no. October 2018, p. 104016, 2019, doi: 10.1016/j.jweia.2019.104016.

[11] I. Kusano, E. Cheynet, J. B. Jakobsen, and J. Snæbjörnsson. (2021). "Aerodynamic study of a suspension bridge deck by CFD simulations, wind tunnel tests and full-scale observations," *IOP Conf. Ser. Mater. Sci. Eng.*, vol. 1201, no. 1, p. 012007, 2021, doi: 10.1088/1757-899x/1201/1/012007.

[12] G. Yao, Y. Chen, Y. Yang, Y. Zheng, L. Wu, and H. Du. (2023). "Research on Mechanism of Vortex-Induced Vibration Railing Effect of Double-Deck Large-Span Suspension Bridge," 2023.

[13] BRITISH STANDARD. (2005). "Eurocode 1 : Actions on structures - Part 1-4: General actions - Wind actions, Committee for Standarization," vol. 3, 2005.

[14] P. B. S. Publication. (2015). "PD 6688-1-4:2015," 2015.

[15] D. J. B. M. Kementrian Pekerjaan Umum dan Perumahan Rakyat. (2022). *PEDOMAN Bidang Jalan dan Jembatan No.02/P/BM/2022*, no. 02. 2022.

[16] SURAT EDARAN MENTERI PEKERJAAN UMUM. (2015). *No. 08/SE/M/2015*. 2015.

[17] American Association of State Highway and Transportation Officials. (2020). *AASHTO LRFD Bridge Design Specifications, 9th EditionOnline Training*. 2020. [Online]. Available:

pISSN 2302-4240
eISSN 2655-2086
Volume 15, Issue 1, March 2026, pp.059-075
DOI: http://dx.doi.org/10.32832/astonjadro.v15i1.19421 http://ejournal.uika-bogor.ac.id/index.php/ASTONJADRO

https://store.transportation.org/item/collectiondetail/202?AspxAutoDetectCookieSupport=1%0Awww.transportation.org